Reappraisal of the Contribution from $[O_2{\cdot}(H_2O)_n]^+$ Cluster Ions to the Chemistry of the Ionosphere

Laurence Angel and Anthony J. Stace*

School of Chemistry, Physics, and Environmental Science, University of Sussex, Falmer, Brighton, U.K. BN1 9QJ

Received: October 27, 1998; In Final Form: February 22, 1999

Presented here are the results of a series of experiments which explore the dissociation patterns of the clusters $[O_2{\cdot}(H_2O)_n]^+$ and $O_4^+{\cdot}H_2O$, where n is in the range 1−5. These clusters have been studied in order to identify reaction channels which may convert O_2^+, as seen in the E-region of the ionosphere, into $H^+(H_2O)_n$ clusters, which are the dominant ions in the lower D-region. Each $[O_2{\cdot}(H_2O)_n]^+$ ion can be viewed as a half-collision intermediate in the sequence of bimolecular hydration reactions, which are thought to lead to the formation of proton hydrates. Three different methods of cluster dissociation have been investigated, unimolecular (metastable) decay, collision-induced fragmentation, and photodissociation by visible laser radiation (450−690 nm). The experiments show that the intermediates $[O_2{\cdot}(H_2O)_n]^+$, for *n* in the range 2−5, preferentially dissociate to form $(H_2O)_n^+$ ions, a route which is largely favored over proton hydrate formation. For the first member of the series, $O_2^+{\cdot}H_2O$, both collisional activation and photoexcitation lead to the appearance of O_2^+ and H_2O as the major fragments. For the trimer, $[O_2{\cdot}(H_2O)_2]^+$, the principal photofragment is $(H_2O)_2^+$ but a significant fraction of H_3O^+ is also observed. Each of the photodissociation channels observed for $O_2^+{\cdot}H_2O$ and $[O_2{\cdot}(H_2O)_2]^+$ exhibits a much wider wavelength dependency than has been observed in previous experiments (Smith, G. P.; Lee, L. C. *J. Chem. Phys.* **1978**, *69*, 5393. Beyer, R. A.; Vanderhoff, J. A. *J. Chem. Phys.* **1976**, *65*, 2313). However, we are able to reproduce these earlier measurements by monitoring the photodissociation of "cold" clusters in the form $O_2^+{\cdot}H_2O{\cdot}Ar$ and $[O_2{\cdot}(H_2O)_2{\cdot}Ar]^+$. A new photodissociation cross section of $(9 \pm 2) \times 10^{-18}$ cm^2 has been determined for the reaction $O_2^+{\cdot}H_2O + h\nu \rightarrow O_2^+ + H_2O$ in the wavelength range 450−690 nm. Taken in conjunction with the solar radiation flux at 87 km, the magnitude of the corresponding unimolecular rate constant (10.8 s^{-1}) suggests that the above process in association with "warm" ions may provide an important sink, which could explain the low $O_2^+{\cdot}H_2O$ ion concentration observed in the ionosphere (McCrumb, J. L. *Planet. Space Sci.* **1982**, *30*, 559). A new rate constant of 2.4 s^{-1} has also been estimated for the photodissociation of "warm" $[O_2{\cdot}(H_2O)_2]^+$ in conjunction with the solar radiation flux at 87 km.

1. Introduction

In the ionosphere, measured ion profiles have detected a clear chemical boundary lying at an altitude of between 82 and 85 km. The nature of this boundary is such that the region above 85 km (the E-region) is dominated by the ions O_2^+, NO^+, and M^+ (where M^+ is either Na^+, Mg^+, Al^+, or Fe^+), whereas below 82 km (the D-region), the dominant ions are of the form $H^+(H_2O)_n$, with $n = 1-8$ being the most abundant.[1,2] The main pathway leading from O_2^+ to the formation of proton hydrates (PHs), $H^+(H_2O)_n$, is assumed to begin with the hydration of O_2^+ via the intermediate ion O_4^+.

$$O_4^+ + H_2O \rightarrow O_2^+{\cdot}H_2O + O_2 \qquad (1)$$

Further hydration is thought to result in one or both of the following reactions being promoted:

$$[O_2{\cdot}(H_2O)_n]^+ \rightarrow H^+(H_2O)_{n-1} + OH + O_2 \qquad (2)$$

or

$$[O_2{\cdot}(H_2O)_n]^+ \rightarrow (H_2O)^+_n + O_2 \qquad (3)$$

$[O_2{\cdot}(H_2O)_n]^+$ ions are presented in this form to acknowledge the fact that, for $n \geq 2$, the position of the positive charge is not well-defined (see below). For each reaction, the equivalent cluster ion can be viewed as the half-collision intermediate in a bimolecular hydration reaction leading to product formation. When $n = 2$, reaction 3 could result in the appearance of two possible isomers of the water dimer ion, $(H_2O)^+_2$, either a disproportionated form, $(H_3O)^+-OH$, or a hydrazine-like ion, $(H_2O-OH_2)^+$. Which of these prevails may depend on the initial structure of the $[O_2{\cdot}(H_2O)_n]^+$ parent ion. A competing reaction channel for all of the $[O_2{\cdot}(H_2O)_n]^+$ ions is the loss of water:

$$[O_2{\cdot}(H_2O)_n]^+ \rightarrow [O_2{\cdot}(H_2O)_{n-1}]^+ + H_2O \qquad (4)$$

Presented here are the results of a detailed investigation into the reactions of $[O_2{\cdot}(H_2O)_n]^+$ cluster ions. Three separate techniques have been used to probe the fragmentation patterns of the ions; unimolecular (metastable) decay and collision-induced fragmentation have been monitored in order to provide evidence of the reaction products anticipated in the above chemical pathways. In addition, we have also investigated the photochemistry of the ions using visible laser radiation in the wavelength range 450−690 nm, and as will be seen, these data

10.1021/jp9841945 CCC: $18.00
Published on Web 04/02/1999

provide evidence of an important loss mechanism, which may account for earlier mass spectrometric measurements of ion number densities.[3]

2. Experiment

Neutral clusters of the form $O_2 \cdot (H_2O)_n$ and $O_4 \cdot H_2O$ were prepared using a "pick-up" technique on an apparatus that consists of a pulsed supersonic nozzle coupled to a modified high-resolution, double-focusing VG ZAB-E mass spectrometer.[4] Argon, at a pressure of approximately 2.5 bar, was directed through a reservoir containing deionized water held at room temperature. The resulting gas−vapor mixture was expanded through a 200 μm diameter conical nozzle into a vacuum chamber to form $Ar \cdot (H_2O)_n$ clusters. The clusters passed through a region containing 10^{-4} mbar of O_2, where collisions resulted in the formation of neutral precursors to the clusters of interest. These then entered the ion source of the mass spectrometer and were ionized by electron impact with 70 eV electrons. To study their fragmentation patterns, each of the cluster ions $[O_2 \cdot (H_2O)_n]^+$ and $O_4^+ \cdot H_2O$ were mass-selected using a magnet and then allowed to travel a further 1.5 m through a field-free region where they underwent either metastable decay, collision-induced dissociation in a gas cell, or photodissociation using a coaxial beam of visible laser radiation. Fragment ions then entered an electrostatic analyzer where they were identified by their kinetic energies, and their relative intensities were monitored using a Daly scintillation detector in association with a photon counter (Stanford Research Systems SR400).

For metastable fragmentation, the time spent travelling in the field-free region, ca. 5×10^{-5} s, is sufficient for cluster ions to undergo a range of unimolecular and internal bimolecular chemical reactions. For these experiments, the background pressure in the flight tube was maintained at $\sim 10^{-8}$ mbar. Collision-induced fragmentation of a parent cluster was promoted by the introduction of a collision gas (air at $\sim 10^{-6}$ mbar) into a cell located in the flight tube between the magnet and electrostatic analyzer. The cell was floated at a potential of −500 V to distinguish collision-induced fragmentation of the parent ions within the collision cell from metastable decay processes occurring outside the cell.

Photodissociation of the cluster ions was promoted using a Spectra Physics MOPO-710 pumped by a Nd:YAG laser. The laser beam was aligned coaxial with the ion beam travelling in the region between the magnet and the electrostatic analyzer. A trigger at 10 Hz from the MOPO was used to pulse the expansion nozzle in the cluster chamber, and a delay was introduced such that the laser beam would interact with the central section of each ion pulse. The photon counter was then gated to acquire photofragmentation signals using foreground−background subtraction to remove contributions due to the metastable decay of ions. Photofragmentation spectra were recorded by scanning the laser under the control of a LabWindows program running on a IBM PC and normalized by simultaneously monitoring the laser power and a measure of the parent ion signal. A typical increment in wavelength was 2 nm, and for each point, photofragment signals were accumulated for between 1000 and 2000 laser shots.

3. Results

a. Metastable Decay. Three major unimolecular decay channels have been identified for $[O_2 \cdot (H_2O)_n]^+$ cluster ions with n in the range 1−5, and the relative intensities of the fragment ions associated with these reactions are shown in Figure 1. The competing loss channels correspond to reactions 2, 3, and 4 given above, and lead to observation of the ions, $H^+(H_2O)_{n-1}$, $(H_2O)_n^+$, and $[O_2 \cdot (H_2O)_{n-1}]^+$, respectively. At $n = 1$, the metastable decay pattern shows a dominant loss of H_2O (85%) through simple bond fission to leave O_2^+. The binding energy of $O_2^+ \cdot H_2O$ has been estimated as $\sim 0.7 \pm 0.1$ eV.[5,6] There is also a small but significant loss of neutral O_2 resulting in the formation of H_2O^+ (15%), which probably arises from a charge-transfer reaction within $O_2^+ \cdot H_2O$ ions. The energy necessary to drive the latter process is small since the difference in ionization energies (IE) is only 0.5 eV (the IE's. of H_2O and O_2 are 12.6 and 12.1 eV, respectively[7]). However, to this must be added the binding energy of $O_2 \cdot H_2O^+$ which again can be considered small, as neutral O_2 is not a good ligand.

As the level of hydration increases ($n \geq 2$), there is a marked change in fragmentation pathway, with $(H_2O)_n^+$ ions becoming the main product (~70% when normalized to the other two loss channels). For $n \geq 2$, the ionization energy of the $(H_2O)_n$ constituent could drop to a point where it, rather than the O_2 molecule, becomes the charge carrier (the ionization energy of the water dimer, $(H_2O)_2$, has been measured as 12.1 eV[8]). Charge transfer to the solvent water molecules would result in parent ions adopting one of two possible forms: either $O_2 \cdot (H_2O)_{n-2} \cdot H_3O^+OH$ or $O_2 \cdot (H_2O)_{n-2}\ (H_2O{-}OH_2)^+$. This in turn would facilitate the loss of O_2 as charge transfer will result in O_2 being the weakest bound ligand in the cluster. The formation of $H^+(H_2O)_{n-1}$ ions, through the loss of O_2 and OH, is comparatively small when compared to the $(H_2O)_n^+$ channel. $H^+(H_2O)_{n-1}$ intensities range from ~10% at $n = 2$ to a maximum of 20% at $n = 4$ and 5. This result is in complete contrast to the $NO^+ \cdot (H_2O)_n$ and $NO_2^+ \cdot (H_2O)_n$ systems, both of which have been the subject of earlier investigations.[9,10] In these examples, PHs are formed via intracluster bimolecular reactions where NO^+ and NO_2^+ ions react with a water molecule to produce the acids HNO_2 and HNO_3, respectively. The remaining proton from the reaction is stabilized by the additional water molecules in the cluster producing the PHs. However, when reactions leading to the formation of proton hydrates occur in the $[O_2 \cdot (H_2O)_n]^+$ system, O_2 and OH are understood to leave the cluster as separate entities. The loss of O_2 may be accompanied by OH loss if the parent ion takes on the form $O_2 \cdot (H_2O)_{n-2} \cdot H_3O^+OH$, and the losses could be sequential if the reaction is preceded by charge transfer.

$$O_2^+ \cdot (H_2O)_n \rightarrow O_2 \cdot (H_2O)_{n-2} \cdot H_3O^+OH \rightarrow (H_2O)_{n-2} \cdot H_3O^+OH + O_2$$

$$H_3O^+OH \cdot (H_2O)_{n-2} \rightarrow H_3O^+ \cdot (H_2O)_{n-2} + OH \qquad (5)$$

b. Collision-Induced MIKE Scans. Results from experiments on the collision-induced dissociation of the $O_4^+ \cdot H_2O$ ion and the $[O_2 \cdot (H_2O)_n]^+$ series for $n = 1-3$ can be seen in Figures 2−5. The higher pressure (10^{-6} mbar) from the introduced collision gas leads to an increase in the dissociation of the cluster ions as they pass through the collision cell. The collision-induced signals are offset from the metastable signals through the application of a small negative voltage to the collision cell. For the most part, the intensities of daughter ions from the collision-induced process are about a factor of 10 larger than the corresponding metastable signals. Although the metastable scan of $O_4^+ \cdot H_2O$ ions showed no conclusive evidence of daughter ions, the collision-induced result shown in Figure 2 yields a very strong signal corresponding to formation of $O_2^+ \cdot H_2O$ from the cluster analogue of reaction 1. This observation is consistent with reaction 1 being the first step in a sequence leading to the

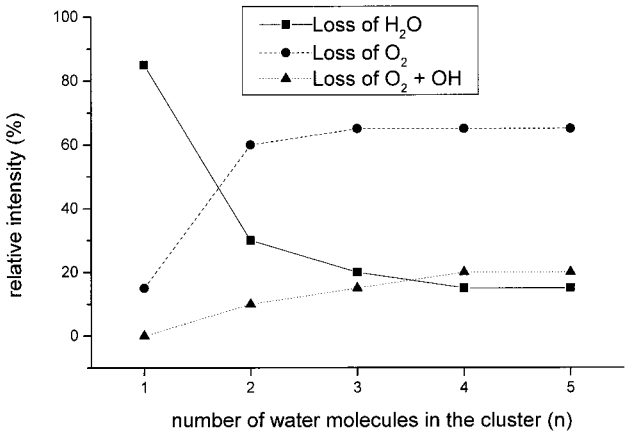

Figure 1. Metastable fragmentation pattern of $[O_2{\cdot}(H_2O)_n]^+$ cluster ions plotted as a function of the number of water molecules in the cluster.

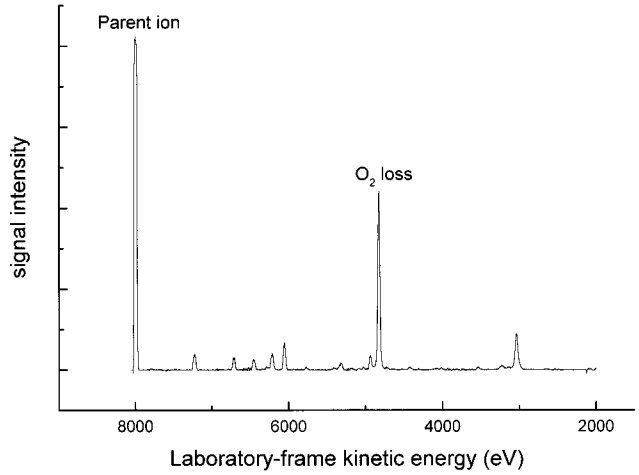

Figure 2. Collision-induced MIKE scan of $O_4^+{\cdot}H_2O$ showing fragmentation ion intensities as a function of laboratory frame kinetic energy.

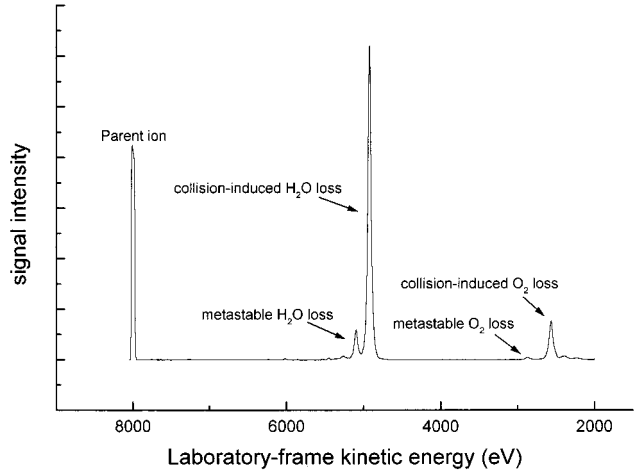

Figure 3. As for Figure 2, but for $O_2^+{\cdot}H_2O$.

formation of $O_2^+{\cdot}(H_2O)_n$ ions.[1] The collision-induced spectrum recorded for the $O_2^+{\cdot}H_2O$ ion (Figure 3) gives very similar results (relative intensities) to those seen in the metastable decay pattern. The spectrum shown has both metastable and collision-induced signals for H_2O and O_2 loss, and these are labeled separately.

Previous experiments[11] on the collision-induced fragmentation of $NO^+{\cdot}(H_2O)_n$ and $NO_2^+{\cdot}(H_2O)_n$ ions found that for clusters

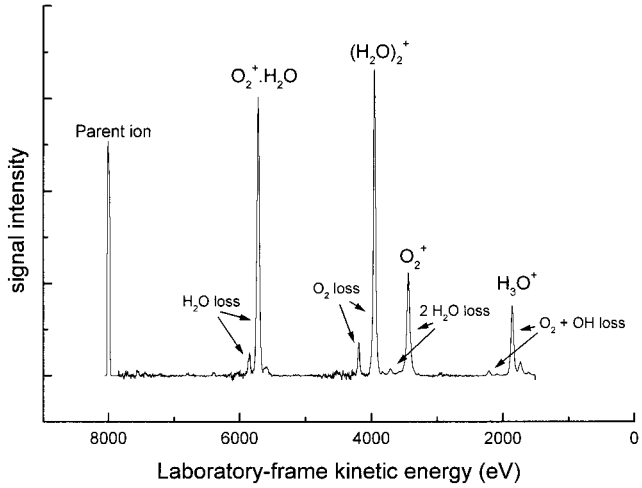

Figure 4. As for Figure 2, but for $[O_2{\cdot}(H_2O)_2]^+$.

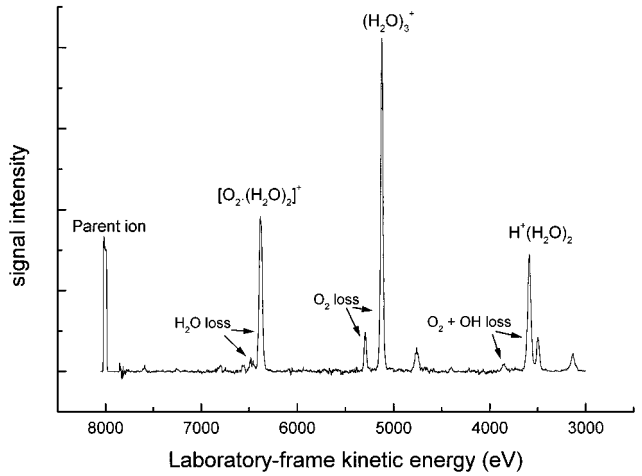

Figure 5. As for Figure 2, but for $[O_2{\cdot}(H_2O)_3]^+$.

at or below the critical hydration size (where proton hydrates are first formed) there was no increase in the loss of either HNO_2 or HNO_3 over and above that observed following metastable decay. This behavior was attributed to proton hydrate formation being dependent on an internal bimolecular reaction driven primarily by solvation rather than internal excitation. In both NO_x^+/water cluster ions, the only reaction pathway found to exhibit an increase as a result of collisional excitation was the loss of H_2O. The analogous critical hydration size for the oxygen/water system is $[O_2{\cdot}(H_2O)_2]^+$, and Figure 4 shows a MIKE scan following the collision-induced fragmentation for this ion. The spectrum does not follow the same pattern observed for the NO_x^+/water clusters. When compared with the metastable signal, $[O_2{\cdot}(H_2O)_2]^+$ exhibits a substantial increase in the collision-induced loss of H_2O, and there is also a relatively large loss of two H_2O. However, where the pattern of behavior does differ significantly from the NO_x^+ systems is in the very substantial increase in both the $(H_2O)_2^+$ and H_3O^+ signals, when compared with their metastable counterparts. There is evidence from both the collision-induced MIKE scan and the metastable decay pattern that charge transfer from O_2^+ to the water dimer may have already taken place, which in turn would facilitate the loss of O_2.

The daughter ion, $(H_2O)_2^+$, could adopt either of the two structures discussed above. However, the loss of O_2 + OH, to give H_3O^+, is increased by the collisional activation, which suggests that either OH is already present in the parent ion in the form $O_2{\cdot}H_3O^+OH$ or that isomerization is promoted by

TABLE 1: Relative Intensities of the Photodissociation Products from Selected Ions Recorded at a Wavelength of 530 nm

parent ion	daughter ions	relative intensity (%)
$O_2^+ \cdot H_2O$	O_2^+	90 (±5)
	H_2O^+	10 (±5)
$O_2^+ \cdot H_2O \cdot Ar$	O_2^+	90 (±5)
	H_2O^+	10 (±5)
$[O_2 \cdot (H_2O)_2]^+$	O_2^+	15 (±10)
	$O_2^+ \cdot H_2O$	5 (±5)
	$(H_2O)_2^+$	50 (±10)
	H_3O^+	30 (±10)
$[O_2 \cdot (H_2O)_2 \cdot Ar]^+$	O_2^+	15 (±10)
	$O_2^+ \cdot H_2O$	5 (±5)
	$(H_2O)_2^+$	50 (±10)
	H_3O^+	30 (±10)

collision. For all higher hydration states, $n = 3-5$, collision-induced fragmentation follows the pattern shown by the metastable decay results in Figure 1. The result for $[O_2 \cdot (H_2O)_3]^+$ is shown in Figure 5.

c. Photodissociation. Photofragmentation spectra were recorded for the clusters $O_2^+ \cdot H_2O$ and $[O_2 \cdot (H_2O)_2]^+$, where the following dissociation pathways were observed in the wavelength range 450−690 nm:

$$O_2^+ \cdot H_2O + h\nu \rightarrow O_2^+ + H_2O \quad (6)$$

$$\rightarrow H_2O^+ + O_2 \quad (7)$$

$$[O_2 \cdot (H_2O)_2]^+ + h\nu \rightarrow (H_2O)_2^+ + O_2 \quad (8)$$

$$\rightarrow H_3O^+ + O_2 + OH \quad (9)$$

The highest photofragmentation yield was recorded for reaction 6. A comparison of the two signals from $O_2^+ \cdot H_2O$ (Table 1) shows that, at ∼530 nm, the percentage formation of O_2^+ and H_2O^+ is approximately the same as that observed in both the metastable and collision-induced processes, where the intensities were O_2^+ (85%) and H_2O^+ (15%). The photofragment yield of O_2^+ as a function of laser wavelength is shown in Figure 6a. A much wider wavelength dependency is exhibited than recorded in previous experiments,[12−14] with photofragmentation being promoted throughout the visible spectrum. The significance of this result will be discussed later. Data were also recorded for the formation of H_2O^+ as a function of laser wavelength (Figure 6b). Again the signal shows a wide wavelength dependency, although the decline is sharper than that seen in Figure 6a, and the signal intensity is almost zero at 690 nm. This latter photofragmentation channel was not seen in previous experiments.

The photodissociation of $[O_2 \cdot (H_2O)_2]^+$ ions proceeds predominantly through the formation of $(H_2O)_2^+$, which is again consistent with the metastable and collision-induced results. The wavelength dependence shown in Figure 7 is again broad, with the photofragment yield reaching a maximum at 530 nm and then decreasing over the range 550−690 nm. When compared with results shown in parts a and b of Figure 6, there is a shift in the maximum to slightly longer wavelengths, and this could be due to two factors: (i) increased solvation of the charge; (ii) a shift in the position of the charge from O_2 to $(H_2O)_2$. Unfortunately, the quality of the spectra recorded for $[O_2 \cdot (H_2O)_2]^+$ do not warrant a detailed interpretation in terms of charge site. The relative intensities of the photodissociation products from $[O_2 \cdot (H_2O)_2]^+$ are shown in Table 1. The results show a small increase in the yield of H_3O^+ via photoexcitation when compared with both the metastable (Figure 1) and collision-induced products (Figure 4). The wavelength dependence of reaction 9 is very similar to that shown in Figure 7. The range of photofragment channels identified here for the $[O_2 \cdot (H_2O)_2]^+$ ion was not recorded in either of the previous studies of this ion.[13,14]

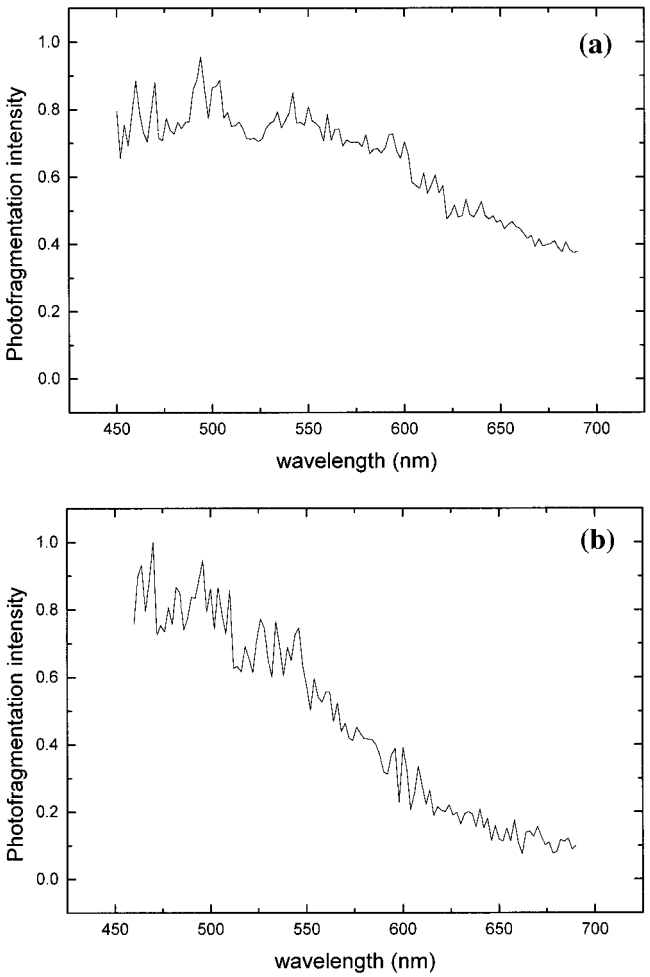

Figure 6. Photofragmentation spectrum recorded for the formation of (a) O_2^+ from $O_2^+ \cdot H_2O$ and (b) H_2O^+ from $O_2^+ \cdot H_2O$.

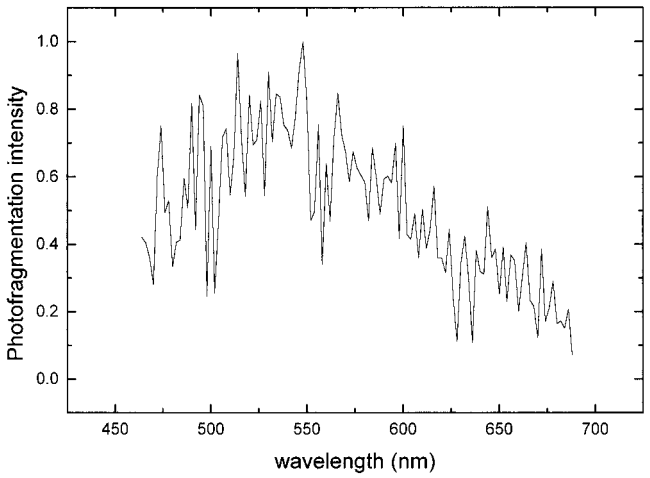

Figure 7. Photofragmentation spectrum recorded for the formation of $(H_2O)_2^+$ from $[O_2 \cdot (H_2O)_2]^+$.

As already noted, the wavelength dependence seen in Figure 6a is quite different from that recorded in earlier experiments.[13,14] A possible reason for the discrepancy is temperature and/or internal energy content; the ions generated by electron impact ionization in these experiments will have internal energies

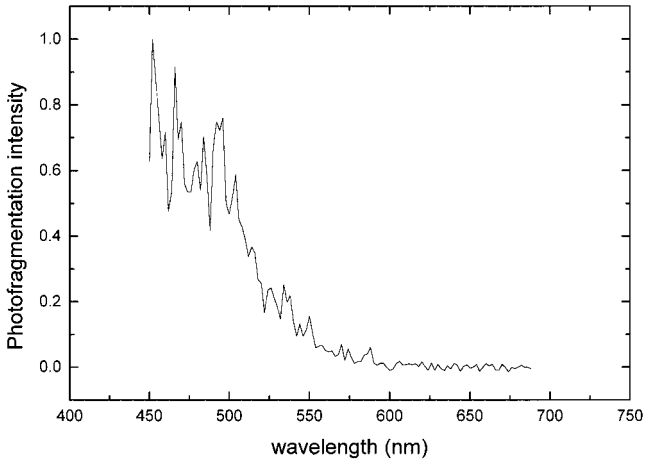

Figure 8. Photofragmentation spectrum recorded for the formation of O_2^+ from $O_2^+{\cdot}H_2O{\cdot}Ar$.

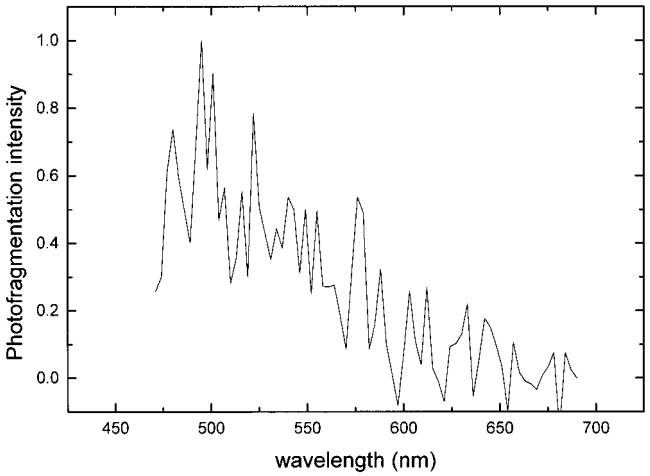

Figure 9. Photofragmentation spectrum recorded for the formation of $(H_2O)_2^+$ from $[O_2{\cdot}(H_2O)_2{\cdot}Ar]^+$.

ranging from almost zero through just above the bond energy for the most facile reaction path (as evidenced by the presence of a metastable signal). In contrast, the cluster ions generated in the experiments by Beyer and Vanderhoff[13] and Smith and Lee[14] were formed by association reactions in drift tubes. Assuming complete collisional relaxation, the ion−molecule products, $O_2^+{\cdot}H_2O$ and $[O_2{\cdot}(H_2O)_2]^+$, were probably formed with internal temperatures close to ambient (300 K).[13,14] In an attempt to study the effect of temperature and/or internal energy, photodissociation spectra were recorded for the ions $O_2^+{\cdot}H_2O{\cdot}$Ar and $[O_2{\cdot}(H_2O)_2{\cdot}Ar]^+$. The rationale being that, in order to retain the weakly bound argon atom, these ions would have to be, on average, "colder" than those studied above.[15] However, the presence of the rare gas atom is not expected to have a significant influence on either the electronic spectra or the relative intensities of photofragments. A spectrum recorded for $O_2^+{\cdot}H_2O{\cdot}Ar$ fragmenting to O_2^+ is shown in Figure 8. When normalized for parent ion intensity, the photofragment yields at ∼500 nm are weaker by a factor of 2 than equivalent data recorded for the $O_2^+{\cdot}H_2O$ cluster. However, the two product ions, O_2^+ and H_2O^+, from $O_2^+{\cdot}H_2O{\cdot}Ar$ are shown in Table 1 to be in exactly the same ratio as that recorded following the photodissociation of $O_2^+{\cdot}H_2O$. The wavelength dependency for the photofragmentation of $O_2^+{\cdot}H_2O{\cdot}Ar$ covers a much narrower range of the spectrum, when compared with that recorded for the $O_2^+{\cdot}H_2O$ cluster, and photofragment signal intensities drop almost to zero at wavelengths greater than 600 nm. Overall, the wavelength dependence recorded for $O_2^+{\cdot}H_2O{\cdot}Ar$ is very similar to that observed previously for $O_2^+{\cdot}H_2O$ ions formed at room temperature.[13,14] This comparison between $O_2^+{\cdot}H_2O$ and $O_2^+{\cdot}H_2O{\cdot}Ar$ shows that temperature (or internal energy content) has a very significant effect on the magnitude of the absorption cross section at particular wavelengths.

Photofragmentation of the $[O_2{\cdot}(H_2O)_2{\cdot}Ar]^+$ cluster yields $(H_2O)_2^+$ as the principal product, and the wavelength dependence of this process is shown in Figure 9. A comparison between spectra recorded for $[O_2{\cdot}(H_2O)_2{\cdot}Ar]^+$ and $[O_2{\cdot}(H_2O)_2]^+$ shows the former to reach a maximum 50 nm to the blue of that seen for the latter. The spectrum recorded for $[O_2{\cdot}(H_2O)_2{\cdot}Ar]^+$ is consistent with spectra recorded previously for $[O_2{\cdot}(H_2O)_2]^+$ ions by Beyer and Vanderhoff[13] and Smith and Lee.[14]

4. Discussion

A series of reaction pathways have been proposed to account for the formation of $H^+(H_2O)_n$ from O_2^+ in the ionosphere.[1,3] Included in the reaction scheme are the intermediates $O_4^+{\cdot}H_2O$, $[O_2{\cdot}(H_2O)_n]^+$, and $(H_2O)_n^+$, all of which have been examined in the experimental results presented here. However, there are evident discrepancies between the reaction products recorded here and what is required to match observations in the ionosphere. Each of the three methods explored for dissociating $[O_2{\cdot}(H_2O)_n]^+$ cluster ions shows that, when $n > 1$, the principle reaction product is $(H_2O)_n^+$, and not the $H^+(H_2O)_m$ ions that have been identified as dominant in the D-region of the ionosphere. As Figure 1 shows, only 20% of reaction products are in the form of $H^+(H_2O)_n$. If the O_2^+ hydration reaction scheme is to make a contribution to the chemistry of the ionosphere, an efficient mechanism is needed to convert $(H_2O)_n^+$ ions into the proton hydrate form $H^+(H_2O)_m$.

Mass spectrometric composition measurements of the lower ionosphere have consistently provided the same positive ion profile[1,2] and show an excellent correlation with NO^+, which is the other dominant ion in the E-region. The critical hydration reactions of NO^+ are with four and five waters and lead to the proton hydrates $H^+(H_2O)_3$ and $H^+(H_2O)_4$. An altitude profile of positive ions in the lower ionosphere region shows that, as NO^+ decreases in concentration, $H^+(H_2O)_3$ and $H^+(H_2O)_4$ ions increase. O_2^+ ions also show a decrease, but at slightly higher altitudes due to the lower critical hydration size required to trigger the formation of water clusters and a charge-transfer reaction between $O_2^+ + NO \rightarrow O_2 + NO^+$. The decrease in concentration of O_2^+ ions correlates closely with observed increases in the number densities of both H_3O^+ and, more markedly, $H^+(H_2O)_2$.[2] These smaller ions cannot be directly accounted for by the NO^+ hydration sequence.[11]

The reaction sequences leading from O_2^+ to ionized water clusters have been reviewed extensively by J. L. McCrumb,[3] and include additional steps to account for the formation of $H^+(H_2O)_2$ ions. One possibility is a ligand switch of the hydroxyl species for an additional water molecule in the $n = 2$ product from reaction 3, as follows:

$$H_3O^+OH + H_2O \rightarrow H_3O^+{\cdot}H_2O + OH \qquad (10)$$

Such a response may depend on $(H_2O)_2^+$ adopting the form H_3O^+OH. Recent calculations on the structure and energetics of ionized water clusters found that the hydrazine-like $(H_2O{-}OH_2)^+$ structure has an energy 0.2 eV lower than that of the isomer H_3O^+OH.[16] Although formation of the $(H_2O{-}OH_2)^+$ configuration via vertical ionization from the equilibrium structure for neutral $(H_2O)_2$ entails surmounting an energy

barrier, that situation may not necessarily apply here. Earlier calculations, however, showed that the hydrazine-like isomer was less stable than the disproportionated ion by 37 kJ mol^{-1}.[17] The collision-induced MIKE spectrum of $[O_2{\cdot}(H_2O)_2]^+$ (Figure 4) suggests the possibility of both forms of the water dimer ion being present as reaction products. HeI photoelectron measurements[8] have determined the vertical ionization potential of $(H_2O)_2$ to be 12.1 ± 0.1 eV, which is exactly the same as that for the O_2 molecule and may help explain the nature of the collision-induced MIKE spectrum of $[O_2{\cdot}(H_2O)_2]^+$. The water loss channels, H_2O and $2H_2O$, could originate from the cluster ion of the form $O_2^+{\cdot}(H_2O)_2$ and the O_2 and O_2 + OH channels from the cluster formed by charge-transfer, $O_2{\cdot}(H_2O)_2^+$, with the water component in the latter adopting one or both of the forms discussed above, i.e., $O_2{\cdot}H_3O^+OH$ or $O_2{\cdot}(H_2O{-}OH_2)^+$. Interestingly, the relative signal intensities arising from the two dissociation pathways are approximately equal, which may be attributed to the near equivalent ionization energies of O_2 and $(H_2O)_2$.

In this final section, we examine how predicted behavior patterns for the chemistry of $[O_2{\cdot}(H_2O)_n]^+$ ions in the ionosphere might be influenced by the alternative absorption profiles determined above. In addition to the formation and loss reactions 1 and 6 for $O_2^+{\cdot}H_2O$ ions in the ionosphere, a further process which contributes to the loss is

$$O_2^+{\cdot}H_2O + H_2O \rightarrow H_3O^+OH + O_2 \qquad (11)$$

A steady-state treatment of reactions 1, 6, and 11 gives an expression for the expected concentration of $O_2^+{\cdot}H_2O$ ions as

$$[O_2^+{\cdot}H_2O] = k_1[O_4^+][H_2O]/(k_6 + k_{11}[H_2O]) \qquad (12)$$

A rate constant of $\sim 1.3 \times 10^{-9}$ cm^3 s^{-1} has been quoted for reaction 1,[18] k_{11} is given as 9×10^{-10} cm^3 s^{-1} [3] and previous measurements of the photodissociation cross section for $O_2^+{\cdot}H_2O$ give k_6 as 0.4 s^{-1}.[19] At an altitude of 87 km, where $O_2^+{\cdot}H_2O$ is formed, H_2O and O_4^+ have concentrations of 6×10^8 cm^{-3} and 8×10^3 cm^{-3}, respectively, which from eq 12 gives a steady-state concentration for $O_2^+{\cdot}H_2O$ of 6640 cm^{-3}.[3] However, the measured $O_2^+{\cdot}H_2O$ ion concentration at 87 km is only 500 cm^{-3}, and previous studies have concluded that there exist no satisfactory rate data to account for the observed deficit.[3] Indeed, McCrumb states that the existing mechanism for the formation of water clusters from O_2^+ is missing an important sink for $O_2^+{\cdot}H_2O$ ions. The photodissociation pathway back to O_2^+ and H_2O offers such a sink, however, the previously measured photodissociation cross section for $O_2^+{\cdot}H_2O$ gives a rate constant[19] which is too low to account for the observed ratios of $O_2^+{\cdot}H_2O$, O_4^+, and O_2^+ in the D-region of the ionosphere.

From the new photofragmentation data presented above, it is clear that internal energy content (or temperature) has a very significant influence on the efficiency of the process $O_2^+{\cdot}H_2O + h\nu \rightarrow O_2^+ + H_2O$ at visible wavelengths. To investigate what influence this result might have on the chemistry of $O_2^+{\cdot}H_2O$ in the upper atmosphere, new photodissociation cross sections for reaction 6 have been estimated from the results presented in Figures 6a and 8. The two parent ion signals, $O_2^+{\cdot}H_2O$ and $O_2^+{\cdot}H_2O{\cdot}Ar$, have been normalized to each other, along with their respective photofragmentation signals leading to O_2^+ ($O_2^+{\cdot}H_2O + h\nu \rightarrow O_2^+ + H_2O$ and $O_2^+{\cdot}H_2O{\cdot}Ar + h\nu \rightarrow O_2^+ + H_2O + Ar$), and the results are plotted in Figure 10a. The previous calculated photodissociation cross-section values[13,14] have been assigned to the $O_2^+{\cdot}H_2O{\cdot}Ar$ spectrum and then rescaled to fit the $O_2^+{\cdot}H_2O$ photofragmentation data, which from the latter gives an estimated cross section of $\sim 1 \times 10^{-17}$ cm^2 for the region 450−600 nm, a value which reduces to $\sim 7 \times 10^{-18}$ cm^2 in the range 600−690 nm. A new rate constant for the reaction $O_2^+{\cdot}H_2O + h\nu \rightarrow O_2^+ + H_2O$ was then calculated from the expression

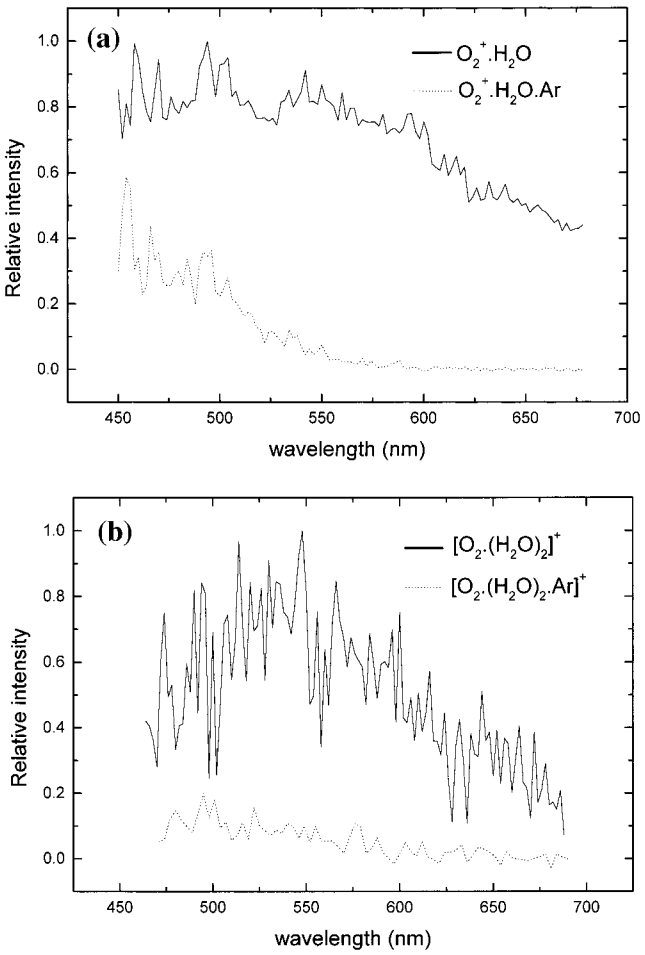

Figure 10. Comparison of photofragmentation spectra recorded for the formation of (a) O_2^+ from $O_2^+{\cdot}H_2O$ and $O_2^+{\cdot}H_2O{\cdot}Ar$ and (b) $(H_2O)_2^+$ from $[O_2{\cdot}(H_2O)_2]^+$ and $[O_2{\cdot}(H_2O)_2{\cdot}Ar]^+$.

$$k_6 = \phi\sigma I \qquad (13)$$

where ϕ is the quantum yield, σ is the average photodissociation cross section of $O_2^+{\cdot}H_2O$ over the wavelength range 450−690 nm (9×10^{-18} cm^2), and I is the total solar radiation flux at these wavelengths at an altitude of 87 km ($\sim 1.2 \times 10^{18}$ photons cm^{-3} s^{-1}).[21] The photodissociation of $O_2^+{\cdot}H_2O$ is considered a single-photon process,[13,14] and assuming that every absorption leads to fragmentation, $\phi = 1$. Therefore, the rate constant for the photofragmentation of "warm" $O_2^+{\cdot}H_2O$ ions is calculated as $k_6 = 10.8$ s^{-1}, a significant increase on the previous value of $k_6 = 0.4$ s^{-1}.[19]

Using the data given above, the calculated steady-state concentration of $O_2^+{\cdot}H_2O$ from eq 12 is estimated to be 550 cm^{-3}, which is very close to the measured value of 500 cm^{-3}. The solar radiation flux into the upper atmosphere is at its peak over the range of visible wavelengths studied in Figure 10a, and falls away rapidly at the UV and near-infrared extremes.[22] Therefore, the photodissociation cross sections estimated here for wavelengths of between 450 and 690 nm probably accounts for a major fraction of the total photofragment yield from $O_2^+{\cdot}H_2O$ ions.

The "warm" $[O_2\cdot(H_2O)_2]^+$ ions also have photodissociation cross sections that are larger than those determined in previous studies. Photofragmentation is complicated, however, by the ion having four photodissociation products, $(H_2O)_2^+$, H_3O^+, O_2^+, and $O_2^+\cdot H_2O$. As shown in Table 1, all the photofragments make a quantitative contribution to the total yield. The most intense photofragment is $(H_2O)_2^+$ (50%), but interestingly, the relative contribution from H_3O^+ (30%) is larger than that seen in either the metastable or collisional activation experiments. Using the procedure outlined above, the photofragment yields of $(H_2O)_2^+$ from $[O_2\cdot(H_2O)_2]^+$ and $[O_2\cdot(H_2O)_2\cdot Ar]^+$ can be scaled to give the results shown in Figure 10b, from which an overall photodissociation cross section for "warm" $[O_2\cdot(H_2O)_2]^+$ clusters is estimated as $\sim 3.5 \times 10^{-18}$ cm^2 at the maximum absorption wavelength (520 nm). This result compares with the previous value of $\sim 1 \times 10^{-18}$ cm^2. If an average cross-section value of 2×10^{-18} cm^2 is used across the visible spectrum, then eq 13 gives a rate constant of $k_8 = \sim 2.4$ s^{-1} for photofragmentation. This new rate constant can be used to estimate a steady-state concentration for $[O_2\cdot(H_2O)_2]^+$ as follows. The important reactions for the formation and loss of $[O_2\cdot(H_2O)_2]^+$ are[3]

$$O_2^+\cdot H_2O\cdot N_2 + H_2O \rightarrow [O_2\cdot(H_2O)_2]^+ + N_2 \qquad (14)$$

$$[O_2\cdot(H_2O)_2]^+ + H_2O \rightarrow (H_2O)_3^+ + O_2 \qquad (15)$$

A steady-state treatment of these reactions together with the photofragmentation step yields an equation for the concentration of $[O_2\cdot(H_2O)_2]^+$ as

$$[O_2\cdot(H_2O)_2]^+ = k_{14}[O_2^+\cdot H_2O\cdot N_2][H_2O]/(k_{15}[H_2O] + k_8) \qquad (16)$$

Earlier studies[3,23] of reactions 14 and 15 have assigned the rate constants as $k_{14} = \sim 10^{-9}$ cm^3 s^{-1} and $k_{15} = \sim 1.8 \times 10^{-9}$ cm^3 s^{-1}, which from eq 16 gives an $[O_2\cdot(H_2O)_2]^+$ concentration of ~ 100 cm^{-3}. At 87 km, mass spectrometric measurements give the $[O_2\cdot(H_2O)_2]^+$ concentration as ~ 400 cm^{-3}, and at 84 km this value is observed to have dropped to ~ 80 cm^{-3}. The value calculated above is of the right magnitude for both of these measurements.

Comparing the results from photofragmentation experiments on $O_2^+\cdot H_2O$ and $O_2^+\cdot H_2O\cdot Ar$, it is quite clear that variations in temperature and/or internal energy content could have a very significant influence on the chemistry of $O_2^+\cdot H_2O$ in the upper atmosphere. Temperatures at altitudes of 90 km, the region called the mesopause, show a very large variability. In the summer, when temperatures are in fact lower than in winter, they can drop to 100 K, while in winter temperatures can be as high as 220 K.[24] An alternative explanation would be to suggest that reactions leading to the formation of $O_2^+\cdot H_2O$ are exothermic and that the rate of collisional relaxation is sufficiently slow as to leave the ion in an excited vibrational state for an extended period of time. A general assumption would appear to be that the sequence of switching reactions proposed to account for the formation of $X^+\cdot H_2O$ (where X is either NO or O_2), leaves the product ion sufficiently stable that subsequent collisions with the background gas reduce the internal energy to a value commensurate with the ambient temperature. However, because the dissociation energy of $O_2^+\cdot H_2O$ is estimated to be 0.7 ± 0.1 eV, the formation of a stable ion need not necessarily imply that the ion is "cold". There is certainly a wealth of dynamical information that would support the possibility of an exchange reaction leaving a polyatomic fragment in a vibrationally excited state.[25]

Given that $O_2^+\cdot H_2O$ might be formed "hot", it is necessary to consider possible relaxation mechanisms. At a pressure of 1 atm, a typical time scale for vibrational−translational (V−T) relaxation is 10^{-4} s.[25] Since both N_2 and O_2 are comparatively inefficient energy transfer agents,[26] the value quoted above can probably be treated as an upper limit; however, cluster ions can be expected to quench faster than neutrals. When account is taken of the reduced pressure characteristic of the ionosphere (at an altitude of ~ 90 km), then the rate constant for V−T relaxation drops to ~ 1 s^{-1}, a value that is slightly larger than the rate constant for the photofragmentation of "cold" $O_2^+\cdot H_2O$ ions (~ 0.4 s^{-1}). In contrast, the rate constant estimate here for reaction 6 is ~ 10 s^{-1}, which is a factor of 10 larger than the estimated relaxation rate constant. Thus, the photofragmentation of nascent $O_2^+\cdot H_2O$ could easily become a competitive loss mechanism, and the only viable relaxation mechanism which may compete with this process is radiative decay.

Acknowledgment. The authors thank EPSRC for financial support and for the award of a studentship to L.A.

References and Notes

(1) Wayne, R. P. *Chemistry of the Atmospheres*; Clarendon Press: Oxford, 1991.
(2) Arnold, F.; Viggiano, A. A. *Planet. Space Sci.* **1982**, *30*, 1295.
(3) McCrumb, J. L. *Planet. Space Sci.***1982**, *30*, 559.
(4) Lethbridge, P. G.; Stace, A. J. *J. Chem. Phys.* **1988**, *89*, 4062.
(5) Howard, C. J.; Bierbaum, V. M.; Rundle, H. W.; Kaufman, F. *J. Chem. Phys.* **1972**, *57*, 3491.
(6) Fehsenfeld, F. C.; Mosesman, M.; Ferguson, E. E. *J. Chem. Phys.* **1971**, *55*, 2115.
(7) Levin, R. D.; Lias, S. G. *Ionization Potential and Appearance Potential Measurements, 1971−1981*; U.S. Department of Commerce, U.S. Government Printing Office: Washington, 1982.
(8) Tomoda, S.; Achiba, Y.; Kimura, K. *Chem. Phys. Lett.* **1982**, *87*, 197.
(9) Stace, A. J.; Winkle, J. F.; Lopez Martens, R. B.; Upham, J. E. *J. Phys. Chem.* **1994**, *98*, 2012.
(10) Stace, A. J.; Winkel, J. F.; Atrill, S. R. *J. Chem. Soc., Faraday Trans.* **1994**, *90*, 3469.
(11) Angel, L.; Stace, A. J. *J. Chem. Phys.* **1998**, *109*, 1713.
(12) Vanderhoff, J. A.; Beyer, R. A. *Chem. Phys. Lett.* **1976**, *38*, 532.
(13) Beyer, R. A.; Vanderhoff, J. A. *J. Chem. Phys.* **1976**, *65*, 2313.
(14) Smith, G. P.; Lee, L. C. *J. Chem. Phys.* **1978**, *69*, 5393.
(15) Ayotte, P.; Bailey, C. G.; Kim, J.; Johnson, M. A. *J. Chem. Phys.* **1998**, *108*, 444.
(16) Barnett, R. N.; Landman U. *J. Phys. Chem.* **1997**, *101*, 164.
(17) Gill, P. M. W.; Radom, L. *J. Am. Chem. Soc.* **1988**, *110*, 4931.
(18) Good, A.; Durden, D. A.; Kebarle, P. *J. Chem. Phys.* **1970**, *52*, 222.
(19) Wisemberg, J.; Kockarts, G. *J. Geophys. Res.* **1980**, *85*, 4642.
(20) Chakrabarty, D. K.; Chakrabarty, P.; Witt, G. *J. Atmos. Terr. Phys.* **1978**, *40*, 437.
(21) Ratcliffe, J. A. *An introduction to the ionosphere and magnetosphere*; Cambridge University Press: New York, 1972; p 10.
(22) Hargreaves, J. K. *The solar-terrestrial environment* Cambridge University Press: New York, 1992; p 135.
(23) Rakshit, A. B.; Warneck, P. *J. Chem. Phys.* **1980**, *73*, 5074.
(24) Plane, J. M. C. *Int. Rev. Phys. Chem.* **1991**, *10*, 55.
(25) Levine, R. D.; Bernstein, R. B. *Molecular Reaction Dynamics and Chemical Reactivity*; Oxford University Press: New York, 1987.
(26) Gilbert, R. G.; Smith, S. C. *Theory of Unimolecular and Recombination Reactions*; Blackwell: Oxford, 1990.